# Transitions, Transients and Evolution

Determination of the accretion disk inner radius taking angular momentum exchange into account

Ali Alpar & Ünal Ertan

(Ertan's model of accretion through a thin disk through different regimes and transitions- applications by the Ertan group; AA: collaborator in some of the applications. References: Attached slides)

## What needs to be explained?

1. Some neutron stars spin-down while accreting, for a wide range of accretion rates (weak propellers, WP).

2. Transitional millisecond pulsars go back and forth between radio ms PSR phases, spinning down with no pulsed X-rays ('strong propellers', SP)
and X-ray ms PSR phases, due to anisotropic accretion, still spinning down as WP, with no radio pulses.

3. Some sources exhibit torque reversals while accreting:
As the accretion luminosity $L_x$ and the mass inflow rate $\dot{M}$ increase/decrease continuously through a critical value, the star switches between spin-down at lower $\dot{M}$ and spin-up at higher $\dot{M}$.
Spin-up (SU) and spin-down rates at either side of this transition are of similar magnitude.

Conventionally, the disk inner radius $r_{in}$ is taken to be the Alfven radius $r_A$, determined by the balance of the magnetic stresses from the neutron star magnetosphere and the material stresses (ram pressure) from the accretion flow:

$$r_{in} \cong r_A \simeq (GM)^{-1/7} \mu^{4/7} \dot{M}^{-2/7}$$

[,$M$ is the neutron star mass, $\dot{M}$ is the mass inflow rate and $\mu$ is the neutron star's dipole magnetic moment.]

The determination of $r_{in} \cong r_A$ does not take rotation into account.

Accretion, with spin-up, is supposed to take place when $r_{in} \leq r_{co} \equiv [\frac{GM}{\Omega_*^2}]^{1/3}$,

while when $r_{in} > r_{co}$ there is no accretion, the matter flowing in through the disk is ejected (propelled out) and the neutron star spins down.

# Accretion is not spherical

Thin disk geometry must be taken into account:

$$\dot{M} = 2\pi r_{in}\, 2h\, \rho\, v_r$$

$\dot{M}$ is the mass inflow rate arriving at the inner disk boundary at $r_{in}$,
$2h$ the disk thickness ; $\rho$ is the mass density and $v_r$ the radial velocity of the mass inflow at $r_{in}$ ,
$v_r = \alpha\, (\frac{h}{r})^2\, r\, \Omega_K(r)$ according to the Shakura -Sunyaev $\alpha$ thin-disk model.

## The interaction of the magnetic field with the disk:

There is a boundary region of width $\Delta r \ll r_{in}$ between the magnetosphere of closed field lines co-rotating with the star at rotation rate $\Omega_*$ and the disk.

The interaction time-scale in the boundary region is $t_{int} \cong |\Omega_* - \Omega_K(r_{in})|^{-1}$; the Kepler rotation frequency in the inner disk being

$$\Omega_K(r_{in}) = [\frac{GM}{r_{in}^3}]^{1/2}.$$

As $t_{int} \ll t_{mag}$, the magnetic diffusion timescale in the highly conducting disk, magnetic field lines move with the magnetosphere, with respect to the disk in the boundary layer,
until $B_\phi \sim B_z$, the field lines reconnect and open-up in the boundary region.

The resulting magnetic torque per unit volume, $\tau_B = \frac{B_\phi B_z}{4\pi}\frac{r}{h} \simeq \frac{B^2}{4\pi}\frac{r}{h}$ spins the neutron star up or down at the rate

$$|\dot{\Omega}| \simeq \frac{|\Omega_* - \Omega_K(r_{in})|}{t_{int}} \simeq |\Omega_* - \Omega_K(r_{in})|^{-2}, \text{ leading to}$$

$$\frac{B^2}{4\pi}\frac{r_{in}}{h} \simeq \rho r_{in}^2 |\Omega_* - \Omega_K(r_{in})|^{-2} = |\omega - 1|^2 (\Omega_K(r_{in}))^2 \text{ in terms of the fastness parameter } \omega \equiv \frac{\Omega_*}{\Omega_K(r_{in})}.$$

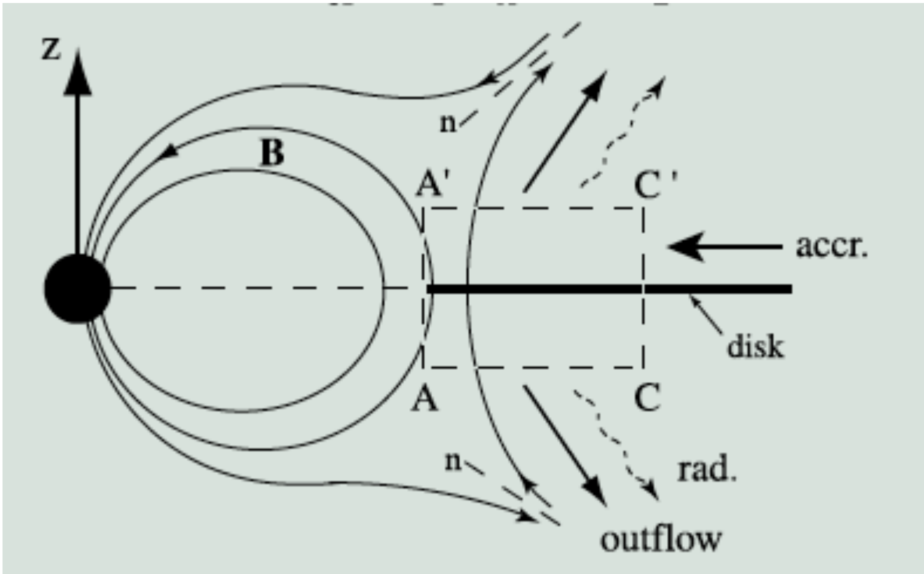

The boundary layer where field lines open-up  (Lovelace et al - 1999)

Putting all this together one can relate the inner radius of the disk to the Alfven radius:

$$r_{in} \simeq 4 \times 10^{-2} \left[ (\omega - 1)^{-2} \, \alpha_{-1} \left( \left[ \frac{h}{r} \right]_{-2} \right)^{2} \right]^{2/7} r_A \qquad (1)$$

where $\alpha_{-1} \equiv (\alpha/0.1)$ and $\left[ \frac{h}{r} \right]_{-2} \equiv \dfrac{\frac{h}{r}}{10^{-2}}$ . (Ertan 2017)

Taking into account the slight dependence of the disk thickness on the parameters,

$$\frac{h}{r} \propto \alpha^{-1} M^{-3/8} \dot{M}^{3/20} r^{1/8},$$

a more detailed formula is obtained (Ertan 2021):

$$R_{\rm in}^{25/8} \, |1 - R_{\rm in}^{-3/2}| \simeq 1.26 \, \alpha_{-1}^{2/5} \, M_{1.4}^{-7/6} \, \dot{M}_{\rm in,16}^{-7/20} \, \mu_{30} \, P^{-13/12}$$

where $R_{\rm in} = r_{\rm in,}/r_{\rm co}$, $\alpha_{-1} = (\alpha/0.1)$, $M_{1.4} = (M/1.4 \, M_\odot)\dot{M}_{\rm in,16} = \dot{M}_{\rm in}/(10^{16} \text{ g s}^{-1})$, $\mu_{30} = \mu/(10^{30} \text{ G cm}^3)$

Torques

$$\Gamma_{total} = \dot{M}\,(GMr_{in})^{1/2} - \frac{\mu^2}{{r_{in}}^3}\left(\frac{\Delta r}{r_{in}}\right) + \Gamma_{dipole}$$

## Lowest $\dot{M}$ : Reaching the escape velocity - The Strong Propeller Regime

All of the inflowing $\dot{M}$ is propelled out of the system. No accretion at all.
The disk is in a steady state: all the mass that flows in is thrown out.

The neutron star acts as a rotation powered pulsar. Radio pulses are generated.
Spin down through the magnetic interaction at the boundary layer as well as the dipole radiation torque.

A low unpulsed X-ray luminosity is generated in the inner disk.

The Strong Propeller regime applies when co-rotating matter in the boundary layer reaches the escape velocity:

$$\Omega_* \, r_{in} = v_{esc}(r_{in}) = \sqrt{2} v_K(r_{in}); \text{ that is, } \Omega_* \equiv \Omega_K(r_{co}) = \sqrt{2}\Omega_K(r_{in}) \;;$$

thus the escape velocity is reached if $r_{in} \geq 2^{1/3} \, r_{co} \cong 1.26 \, r_{co}$ .

## Intermediate $\dot{M}$ : the escape velocity is not reached - The Weak Propeller Regime

When $r_{co} < r_{in} < 2^{1/3}\, r_{co}$ , inflowing $\dot{M}$ arriving at $r_{in}$ is not thrown out. It returns to the disk, causing a pile up, which pushes the inner disk inwards until $r_{\rm in} = r_{\rm co}$. This starts the accretion onto the NS. —> Transition into the **weak propeller (WP).**

The magnetic interaction torques are dominant, leading to spin down.

The neutron star acts as an accretion powered X-ray pulsar. There are no radio pulses as the accretion flow into the magnetosphere quenches pulsed radio emission.

## High $\dot{M}$ : Accretion with Spin-up

At higher $\dot{M}_{\rm in}$ the inner disk can penetrate inside $r_{\rm co}$ when the viscous stresses dominate the magnetic stresses, which occurs approximately when $r_{\rm in} \simeq r_{\rm A} \simeq r_{\rm co}$ . The boundary region where $B_\phi$ caused spin-down is quenched.

This is the transition from the WP to the **spin-up (SU) phase (torque reversal)**:
The angular momentum transfer by accreting matter spins the neutron star *up*.

The neutron star acts as a high luminosity accretion powered X-ray pulsar.

## The inner disk radius

$$r_{in} \simeq 4 \times 10^{-2} \left[ (\omega - 1)^{-2} \, \alpha_{0.1} \left( \left[ \frac{h}{r} \right]_{-2} \right)^2 \right]^{2/7} r_A. \qquad (1)$$

This formula is strictly valid in the SP phase.The fastness parameter $\omega \equiv \frac{\Omega_*}{\Omega_K(r_{in})} = (\frac{r_{in}}{r_{co}})^{3/2}$.

In the Strong Propeller Regime in the $\omega \gg 1$ limit

$$r_{in} \simeq 0.17 \left[ \alpha_{-1}^{2/13} \left( \left[ \frac{h}{r} \right]_{-2} \right)^{4/13} \right] {r_{co}}^{6/13} \, {r_A}^{7/13} \sim (r_{co} \, r_A)^{1/2} \ll r_A \,.$$

In the accretion with spin-up regime, $\omega < 1$, $r_{in} < r_{co}$.

Near the SU-WP transition (spin-up -spin-down transition with accretion), $\omega \cong 1$, we have

$$r_{in} \cong r_{co} \simeq r_A$$

## Critical $\dot{M}$ for the transitions between SP, WP and SU Regimes

The SP regime applies when $\dot{M} < \dot{M}_{SP-WP} \simeq 4 \times 10^{12}\ gm\ s^{-1}\ \alpha_{-1}\ P(ms)^{-7/3}\ (\mu_{26})^2\ \left(\frac{h}{r}\right)^2_{-2}$.

The WP regime applies when $\dot{M}_{WP-SU} > \dot{M} > \dot{M}_{SP-WP}$.

The accretion with spin-up regime applies when $\dot{M} > \dot{M}_{WP-SU} \simeq 2 \times 10^{17}\ gm\ s^{-1} \left(\frac{M}{M_\odot}\right)^{5/3} (\mu_{26})^2\ P(ms)^{-7/3}$,

obtained by setting $r_{co} \simeq r_A$.

# ROTATIONAL PHASES

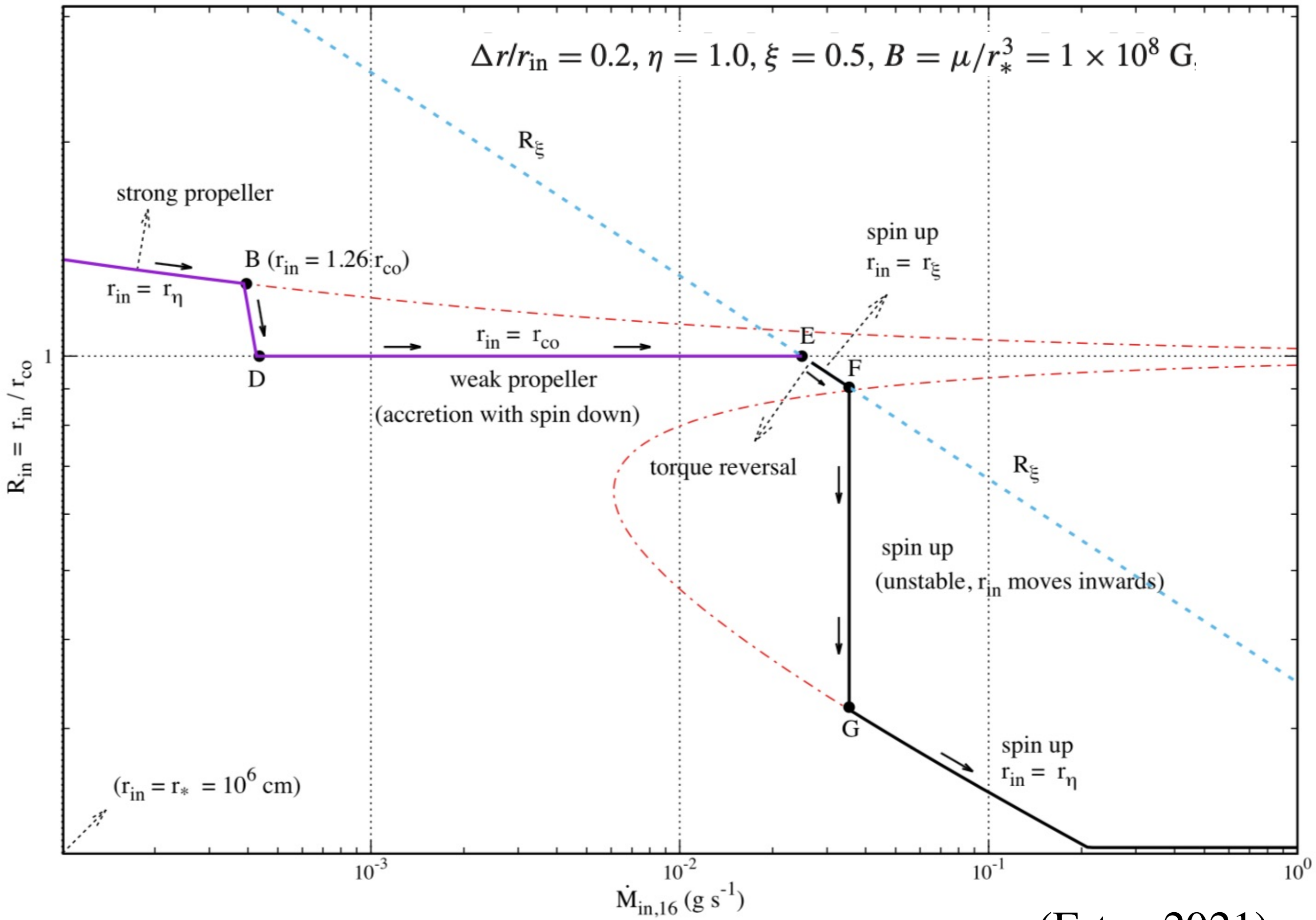


(Ertan 2021)

(a)

# The Model Explains

1. That some neutron stars indeed spin-down while accreting, as weak propellers, WP, for a wide range of accretion rates

$$\dot{M}_{SP-WP} \sim 10^{12} gm\ s^{-1} < \dot{M} < \dot{M}_{WP-SU} \sim 10^{16} gm\ s^{-1}.$$

2. Transitional millisecond pulsars go back and forth between radio ms PSR phases, spinning down with no pulsed X-rays ('strong propellers', SP, with $L_x = L_{disk} = \dfrac{GM\dot{M}}{2r_{in}}$ and X-ray ms PSR phases, still spinning down as WP, with no radio pulses.

3. Some sources exhibit torque reversals while accreting:
As the accretion luminosity $L_x$ and the mass inflow rate $\dot{M}$ increase/decrease continuously through a critical value, the star switches between spin-down at lower $\dot{M}$ and spin-up at higher $\dot{M}$ with small changes in $\dot{M}$.

Spin-up (SU) and spin-down (WP) rates at either side of this transition are of similar magnitude.

4. For most LMXBs the inner radius of the disk calculated with this model is found to extend down to the neutron star surface, explaining why most LMXBs are not millisecond X-ray pulsars - simply because the magnetosphere that directs the pulsed radiation is quenched out of existence.

5. Applications to the evolution of young neutron stars with fallback disks, with $r_{in}$ and torques calculated by this model explains the evolutionary connections and populations on the $P - \dot{P}$ diagram.

# APPLICATION TO TORQUE REVERSALS of 4U 1626-27 (LMXB)

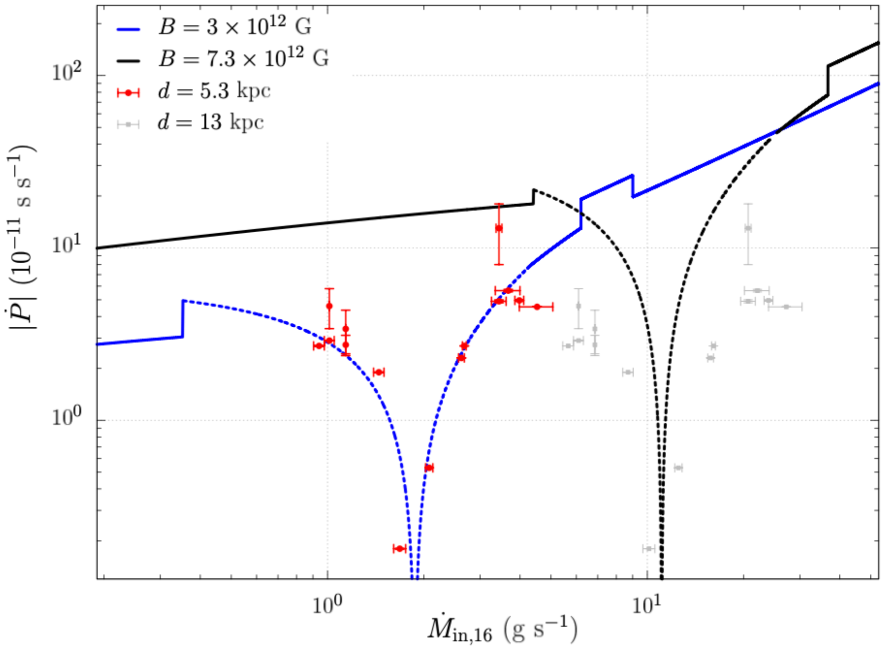


**Fig. 2.** Illustrative model curves with torque-reversals corresponding to $\dot{M}_{\rm in}$ values. The blue model curve is the same as given in Fig. 1b ($\Delta r/r_{\rm in} = 0.2$ , $\eta = 1$ and $\xi = 0.8$). The black curve is also obtained with the same disk parameters, but for a larger distance that requires a stronger $B$ and a higher $\dot{M}_{\rm in}$ during the torque reversal. The magnetic field $B$ and distance $d$ values used in the models are given in the figure. It is clearly seen that the model with the larger $d$ cannot reproduce the data (grey data points).

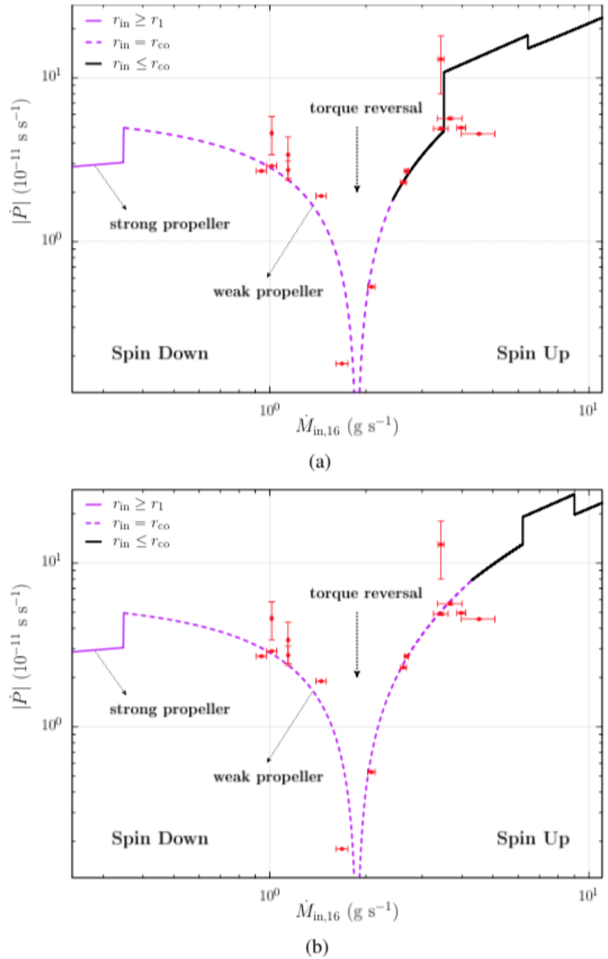


**Fig. 1.** Torque reversal of 4U 1626–67 for different $\xi$ values. The model parameters are $B = 3 \times 10^{12}$ G, $\Delta r/r_{\rm in} = 0.2$, $\eta = 1$, $d = 5.3$ kpc. We obtained the data from Takagi et al. (2016, and references therein). For both models, the spin-down torque is inactivated when $r_{\rm in} = r_{\rm co} - \Delta r/2$ (see the text for details). (a) $\xi = 0.68$, (b) $\xi = 0.80$.

# References


- Calculation of the inner disk radius in the SP phase and the SP/WP transition (Ertan 2017)

- Application to the torque variation of t-MSPs (Ertan 2018)

- Extension of the model to the torque reversals (WP/SP transition) and the SU phase (Ertan 2021)

- Application to the torque reversals of 4U 1626-67 (Gençali, Niang, Toyran, Ertan, Ulubay, Şaşmaz, Devlen, Vahdat, Özcan & Alpar 2022)

- Lack of pulsations from LMXBs (Niang, Ertan, Gençali, Toyran, Ulubay, Devlen, Alpar & Gügercinoğlu 2024)

- Long-term evolutionary links between the isolated neutron star populations (Gençali & Ertan 2024)

- Binary and neutron star evolution in low-mass X-ray binaries on the evolutionary tracks of accreting millisecond X-ray pulsars (Niang, Ertan, Gençali, Ertuğrul, Ulubay, Devlen & Alpar 2026)

- The torques acting on accreting millisecond X-ray pulsars in the outburst and quiescent states, and during the long-term evolution (Ertuğrul, Gençali & Ertan, 2026)

References - Early developments:

the diffusion time-scale of the field lines is much longer than the dynamical time-scale of the disc, $\tau_{\mathrm{dyn}} \sim \Omega_{\mathrm{K}}^{-1}$, where $\Omega_{\mathrm{K}}$ is the Keplerian angular speed (Aly 1985; Wang 1987; Lovelace, Romanova & Bisnovatyi-Kogan 1995; Hayashi, Shibata & Matsumoto 1996; Miller & Stone 1997; Uzdensky, Konigl & Litwin 2002; Uzdensky 2004; Fromang & Stone 2009).

Detailed simulations suggest that the magnetic field lines interact with the inner disc in a narrow boundary layer (Lovelace et al. 1995; Hayashi et al. 1996; Miller & Stone 1997). The closed field lines interacting with the matter inflate and open up within a short interaction time-scale $\tau_{\rm int} = |\Omega_* - \Omega_{\rm K}(r_{\rm in})|^{-1}$. In the propeller phase, the matter in the boundary layer can be thrown out along the open field lines. Subsequently, the field lines reconnect on a time-scale $\tau_{\rm dyn}$ (Lovelace et al. 1999; Ustyugova et al. 2006). This interaction boundary is at the innermost region of the disc with a narrow radial extension ($\Delta r < r$). Inside $r_{\rm in}$, the field lines are closed and rotate together with the matter, forming the magnetosphere. Using the basic results of the model proposed by Lovelace et al. (1999), Ertan (2017) proposed a model to calculate $r_{\rm in}$ in the propeller phase, and the critical condition for the onset of the propeller mechanism. The model was later extended to cover all the rotational phases and the critical conditions for the transitions between these phases (Ertan 2021) and was utilized to account for the torque reversals of 4U 1626–67 (Gençali et al. 2022). We will use the